

Pure Odd Frequency Superconductivity at the Cores of Proximity Vortices

Mohammad Alidoust,¹ Alexander Zyuzin,^{2,3} and Klaus Halterman⁴

¹*Department of Physics, Faculty of Sciences, University of Isfahan, Hezar Jerib Avenue, Isfahan 81746-73441, Iran*

²*Department of Theoretical Physics, The Royal Institute of Technology, Stockholm, SE-10691 Sweden*

³*A. F. Ioffe Physical - Technical Institute, 194021 St. Petersburg, Russia*

⁴*Michelson Lab, Physics Division, Naval Air Warfare Center, China Lake, California 93555, USA*

(Dated: February 17, 2022)

After more than a decade, direct observation of the odd frequency triplet pairing state in superconducting hybrid structures remains elusive. We propose an experimentally feasible setup that can unambiguously reveal the zero energy peak due to proximity-induced *equal spin* superconducting triplet correlations. We theoretically investigate a two dimensional Josephson junction in the *diffusive* regime. The nanostructure consists of a normal metal sandwiched between two ferromagnetic layers with spiral magnetization patterns. By applying an external magnetic field perpendicular to the junction plane, vortices nucleate in the normal metal. The calculated energy and spatially resolved density of states, along with the pair potential, reveal that remarkably, only triplet Cooper pairs survive in the vortex cores. These isolated odd frequency triplet correlations result in well defined zero energy peaks in the local density of states that can be identified through tunneling spectroscopy experiments. Moreover, the diffusive regime considered here rules out the possibility of Andreev bound states in the vortex core as contributors to the zero energy peaks.

PACS numbers: 72.10.-d, 72.10.Bg, 73.63.-b, 73.25.+i, 74.78.-w

Introduction. In analogy to the pairing mechanism in ³He, spin triplet Cooper pairing was predicted to coexist with spin singlet correlations in hybrid structures consisting of *s*-wave superconductors (S) and inhomogeneous ferromagnets (IFMs) [1–12]. For these types of systems, spin triplet correlations with nonzero (± 1) projections along a given spin quantization axis can result in long range proximity effects [1, 2]. It was argued that traces of the triplet pairing state could be revealed in measurements of the critical supercurrent [1–3, 6, 9, 11, 13–17] and local density of states (LDOS) [18–21]. In the former case, the critical supercurrent should show a slow damping behavior as a function of spin singlet depairing factors (such as the thickness of a uniform magnetic layer), while in the later case, the LDOS should exhibit a peak at zero energy. Unfortunately, an unambiguous and direct observation of the spin triplet pairing state in F/S hybrid platforms remains elusive due to the difficulty in isolating the triplet pairs entirely, even when a half-metallic ferromagnet is incorporated [8, 9, 20, 22–24]. Thus, it is preferable to find a practical way to manipulate the pair correlations so that the singlet and triplet components occupy separate regions of space. In contrast to current approaches [1, 2, 8–11, 14, 15, 19–24], controlling the pair correlations in this way can be achieved by applying a magnetic field to the F/S structure [11], inducing proximity vortices with normal state cores. This may consequently create a favorable situation where the singlet and triplet pair correlations can be fully separated at the vortex cores.

The first experimental observation of nonmagnetic proximity induced vortices recently occurred in two dimensional normal metal (N) Josephson junctions [25]. It was observed that applying an external magnetic field

perpendicular to a wide SNS Josephson junction causes nucleation of a vortex lattice in the normal metal parallel to the SN interfaces. The number of induced vortices depends on the intensity of the externally applied magnetic field. The proximity-induced vortices in two dimensional Josephson structures was first discussed theoretically in connection with the Fraunhofer and anomalous critical supercurrent responses in Josephson junctions with both normal metal [26, 27] and ferromagnetic elements [11]. This concept was also recently extended to disordered surface states of topological insulators and Dirac materials in the quasiclassical regime [28].

In this paper, we study the *diffusive* S-Ho/N/Ho-S Josephson junction structure shown in Fig. 1 as a system for fully isolating the odd frequency spin-1 superconducting triplet correlations. The existence of the triplet pairs is directly revealed in the form of DOS signatures. The role of the Holmium (Ho) layers is that of a spin-1 triplet pairing source, while the superconducting phase gradient across the junction drives the triplet pairs into the N region. By taking advantage of the fact that an external magnetic field applied perpendicularly to the junction plane induces vortices in the N region, while expelling the spin singlet pairs from the vortex centers (creating a normal core), we demonstrate that spin-1 triplet correlations occupy the normal core region, as revealed through peaks in the zero energy DOS. We support our findings by a spin parameterization technique to the Green function of system that allows for fully identifying the behavior of each individual pair correlation [11]. Since the N layer is a diffusive metal with numerous strong scattering sources, the superconducting coherence length is much larger than the mean free path, and therefore bound states cannot form at the centers of the vortices,

ruling out Andreev bound states as contributors to the zero energy peak (ZEP). Consequently, the spin-1 triplet channel is highly dominant within the vortex core, causing the ZEP in the DOS.

Results and Discussions. It is now firmly established that the electronic properties of a diffusive hybrid superconducting structure can be described by the Usadel equation within the quasiclassical framework [1, 2, 13]. The Usadel equation in the normal region reads [29]:

$$D\hat{\nabla}(\hat{G}\hat{\nabla}\hat{G}) + i[\varepsilon\hat{\rho}_z, \hat{G}] = 0, \quad \hat{G}(\varepsilon, \mathbf{R}) = \begin{pmatrix} G^A & G^K \\ 0 & G^R \end{pmatrix}, \quad (1)$$

where D represents the diffusion constant in the N and S regions and ε is the quasiparticle energy measured from the Fermi level. We normalize all lengths by the superconducting coherence length, $\xi_S = \sqrt{\hbar D/|\Delta_0|}$, energies by the superconducting gap at zero temperature, $|\Delta_0|$, and adopt natural units where $\hbar = k_B = 1$. The Green function $\hat{G}(\varepsilon, \mathbf{R})$ is composed of the advanced, $G^A(\varepsilon, \mathbf{R})$, retarded, $G^R(\varepsilon, \mathbf{R})$, and Keldysh, $G^K(\varepsilon, \mathbf{R})$, propagators, which carry the complete physical information of the system considered. In the presence of an external magnetic field, $\mathbf{H} = (0, 0, H_z)$, directed perpendicular to the junction plane, the derivatives can be replaced by their covariants, i.e. $\hat{\nabla} = \nabla - [ie\mathbf{A}\hat{\rho}_z, \dots]$. Here \mathbf{A} is the vector potential associated with the external field \mathbf{H} . In equilibrium, as considered throughout the paper, the advanced and Keldysh propagators can be expressed via the Retarded Green function. In this case, one can show that $G^A(\varepsilon, \mathbf{R}) = -\{\hat{\rho}_z G^R(\varepsilon, \mathbf{R}) \hat{\rho}_z\}^\dagger$ and $G^K(\varepsilon, \mathbf{R}) = \{G^R(\varepsilon, \mathbf{R}) - G^A(\varepsilon, \mathbf{R})\} \tanh(\varepsilon k_B T/2)$, where k_B is the Boltzmann constant, and the system temperature is denoted by T . Therefore, it suffices to focus on the retarded Green function, and then eventually construct the total propagator using the simple relations above. One useful limit for F/S structures is the so-called low proximity limit. This limit permits linearization of the Green function, yielding a linear set of differential equations that are in general coupled [11, 28]. Although highly useful transport characteristics can be captured in this limit, the full proximity regime allows for the study of energy-resolved and spatially-resolved DOS, and other relevant physical quantities. Hence, we first employ the full proximity limit, resulting in a complex set of nonlinear coupled differential equations [11] and then complement our findings with a spin parameterization technique in the low proximity limit.

In establishing a numerically stable algorithm in the *full* proximity limit, we use the so-called Riccati parametrization [30], where it is convenient to introduce two correlated functions γ and $\tilde{\gamma}$, which are in effect unknown 2×2 matrices. In this parameterization scheme, the retarded Green function takes the following form:

$$G^R(\varepsilon, \mathbf{R}) = \begin{pmatrix} (1 - \gamma\tilde{\gamma})\Gamma & 2\gamma\tilde{\Gamma} \\ 2\tilde{\gamma}\Gamma & (\tilde{\gamma}\gamma - 1)\tilde{\Gamma} \end{pmatrix}, \quad (2)$$

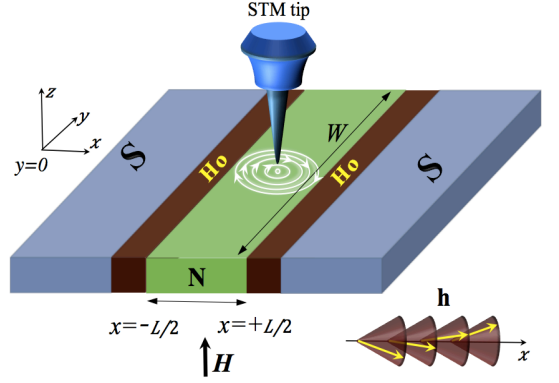


FIG. 1. (Color online) Schematic of the S-Ho/N/Ho-S junction subject to a perpendicular external magnetic field \mathbf{H} . The junction plane resides in the $z = 0$ plane and the N/Ho interfaces are located at $x = \pm L/2$. The junction has a length and width of L and W , respectively. The two helimagnets (Holmium type) with internal fields \mathbf{h} (see text) are attached to the diffusive normal metal (N) solely for producing spin-1 triplet pair correlations. The perpendicular external magnetic field induces proximity vortices in the N region depicted schematically.

in which $\Gamma = (1 + \gamma\tilde{\gamma})^{-1}$ and $\tilde{\Gamma} = (1 + \tilde{\gamma}\gamma)^{-1}$. Substituting the Riccati parameterized Green function into the Usadel equation, Eq. (1), and considering the external magnetic field, we arrive at the following equations for γ and $\tilde{\gamma}$ in the N region of Fig. 1:

$$\partial_{k,k'}^2 \gamma - 2(\partial_{k,k'} \gamma) \tilde{\gamma} \Gamma \partial_{k,k'} \gamma - (2eH_z k')^2 \{2\Gamma - 1\} \gamma - 4ieH_z k' \left\{ \partial_k \gamma - (\partial_k \gamma) \tilde{\Gamma} - \Gamma \partial_k \gamma \right\} = -2i \frac{\varepsilon}{D} \gamma, \quad (3a)$$

$$\partial_{k,k'}^2 \tilde{\gamma} - 2(\partial_{k,k'} \tilde{\gamma}) \gamma \tilde{\Gamma} \partial_{k,k'} \tilde{\gamma} - (2eH_z k')^2 \{2\tilde{\Gamma} - 1\} \tilde{\gamma} + 4ieH_z k' \left\{ \partial_k \tilde{\gamma} - (\partial_k \tilde{\gamma}) \Gamma - \tilde{\Gamma} \partial_k \tilde{\gamma} \right\} = -2i \frac{\varepsilon}{D} \tilde{\gamma}. \quad (3b)$$

For compactness, we have defined $k \equiv x$ and $k' \equiv y$ for the spatial coordinates so that $\partial_{k,k'} \equiv \partial_x + \partial_y$. We have also employed the Coulomb gauge, so that $\nabla \cdot \mathbf{A} = 0$.

We consider a realistic situation where the junctions are well described by a tunneling process [31]. The appropriate boundary conditions for this regime are the Kupriyanov-Zaitsev boundary conditions [31]:

$$\zeta \hat{\mathbf{g}} \mathbf{n} \cdot \hat{\nabla} \hat{G} = [\hat{G}, \hat{G}_S], \quad G_S^R = \begin{pmatrix} \mathcal{C} & \mathcal{S} e^{+i\varphi} \\ \mathcal{S} e^{-i\varphi} & -\mathcal{C} \end{pmatrix}, \quad (4)$$

where ζ is the ratio of the barrier resistance to the resistivity of the normal layer, and the components of the retarded superconducting bulk solution [31], can be expressed by $\mathcal{C} \equiv \cosh \theta \sigma_0$ and $\mathcal{S} \equiv i \sinh \theta \sigma_y$, in which $\theta = \text{atanh}(\Delta/\varepsilon)$. The superconducting phase is denoted by φ and the unit vector normal to the interfaces is denoted by \mathbf{n} . Inserting the Riccati parameterized Green function into the boundary conditions, Eq. (4), we find the following first order differential equations at

$x = \mp L/2$ with $\varphi = \pm\phi/2$:

$$\partial_k \gamma + 2ieH_z k' \gamma = \pm(2\frac{\mathcal{C}}{\mathcal{S}} + \gamma e^{\mp i\phi/2} - \frac{e^{\pm i\phi/2}}{\gamma}) \frac{\mathcal{S}\gamma}{\zeta}, \quad (5a)$$

$$\partial_k \tilde{\gamma} - 2ieH_z k' \tilde{\gamma} = \pm(2\frac{\mathcal{C}}{\mathcal{S}} + \tilde{\gamma} e^{\pm i\phi/2} - \frac{e^{\mp i\phi/2}}{\tilde{\gamma}}) \frac{\mathcal{S}\tilde{\gamma}}{\zeta}. \quad (5b)$$

Next, to generate spin-1 triplet correlations and have them occupy the N region, several practical ways can be considered [9]. For example, the triplets can be generated in a SF/N/FS type junction with the aid of uniform noncollinear magnets, or texturized magnets [9, 11]. Another option would be the use of spin-active interfaces in the form of magnetic insulators or materials with strong spin-orbit coupling in the presence of a Zeeman field [9]. Nonetheless, we emphasize that there are a number of ways to generate spin-1 triplet correlations that would yield essentially the same results presented here. Therefore, to simplify the setup and proposed experiment, we consider the structure sketched in Fig. 1, with the assumption that the spin-1 triplet correlations have been induced in the N region by the Holmium (Ho) layers which can be described by additional terms $(\mathbf{h} \cdot \boldsymbol{\sigma})\gamma - \gamma(\mathbf{h} \cdot \boldsymbol{\sigma}^*)$, and $\tilde{\gamma}(\mathbf{h} \cdot \boldsymbol{\sigma}) - (\mathbf{h} \cdot \boldsymbol{\sigma}^*)\tilde{\gamma}$ in the Usadel equation Eq. (3a) and (3b), respectively. One can also solve the Usadel equation (1) without the kinetic part and derive new solutions to the bulk superconductors in the presence of an inhomogeneous magnetization, the effect of which is to renormalize \hat{G}_S in Eq. (4), including the \mathcal{C} and \mathcal{S} terms. The Holmium-like magnetization pattern is coordinate dependent and can be described by $\mathbf{h} = h_0(\cos \psi, \sin \psi \sin \beta x/a, \sin \psi \cos \beta x/a)$, in which ψ and β are the apex and azimuthal angles of the cone that constitutes the spiral pattern (see Fig. 1), and a is the atomic interlayer distance [32]. Here we take the widely used values, $\psi = 4\pi/9$ and $\beta = \pi/6$ [32].

To determine the signatures of various proximity induced superconducting correlations, we calculate the singlet pair potential U_{pair} :

$$U_{pair}(\mathbf{R}) = -\frac{\mathcal{N}_0 \lambda}{8} \text{Tr} \left\{ \frac{\rho_x - i\rho_y}{2} \tau_z \int d\varepsilon G^K(\varepsilon, \mathbf{R}) \right\}, \quad (6)$$

and the local density of states:

$$\mathcal{N}(\varepsilon, \mathbf{R}) = \frac{\mathcal{N}_0}{2} \text{Re} \left[\text{Tr} \{ \hat{G}(\varepsilon, \mathbf{R}) \} \right], \quad (7)$$

where \mathcal{N}_0 is the density of states per spin at the Fermi level and λ is the pairing interaction constant.

To begin, we present the local DOS and pair potential in Fig. 2 for the case $h_0 = 0$, i.e. the Ho layers in Fig. 1 have been replaced with normal metals, and consequently no triplet correlations exist. To further simplify our analysis, we consider a sufficiently wide junction, $W \gg L$, and set the external magnetic field so that only a single magnetic flux quantum Φ_0 passes through the N region. We also assume representative values of $\zeta = 4$, the system

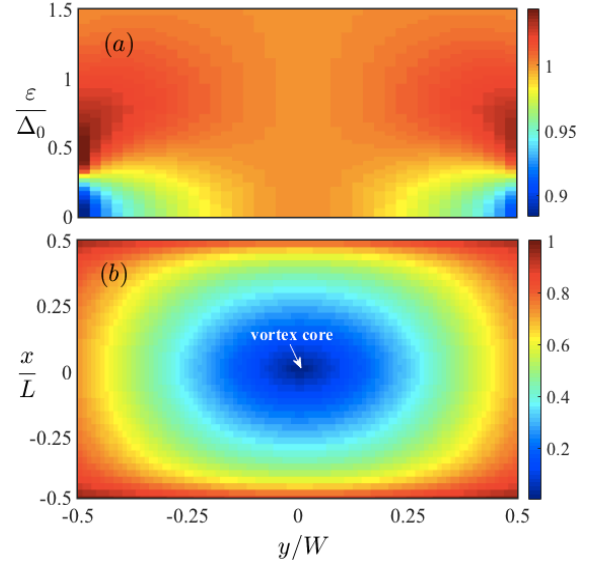


FIG. 2. (Color online) (a) Color map of normalized local density of states as a function of quasiparticles' energy ε and location along the junction width y at $x = 0$ inside the diffusive normal metal N when the outer Ho layers are off i.e. $h_0 = 0$. (b) Corresponding spatial map of normalized singlet pair potential.

temperature set at $T = 0.05T_c$ (with critical temperature T_c), and a superconducting phase difference $\phi = \pi$. This choice of ϕ only shifts the vortex core to $x = y = 0$ [11, 28] without affecting the final outcome. Due to the single magnetic quantum flux in N, a single proximity vortex is induced [26]. As seen in panel (b), the pair potential vanishes at $x = y = 0$, coinciding with the normal core of the vortex. To shed more light on the influence of proximity effects on the vortex behavior, we have also calculated the corresponding LDOS shown in panel (a) as a function of the quasiparticle energy, ε , and location along the junction width, y (at $x = 0$). It is apparent that the LDOS at $x = y = 0$ is equal to unity which clearly demonstrates that no singlet superconducting correlation exist in the vicinity of $x = y = 0$, where the singlet pair potential is zero. Note that U_{pair} only involves the spin singlet component of the Green function even in the presence of an external magnetic field. This can be clearly seen in the low proximity regime where the contributions from the singlet and triplet channels can be decomposed [11]. Panel (a) shows that the LDOS becomes reduced at locations away from $x = y = 0$. This can be understood by noting that the *singlet* pair correlations are responsible for inducing a minigap in the hybrid structure. This is reflected in the behavior of the pair potential [panel (b)] which shows that U_{pair} increases as one moves away from the normal core of vortex ($x = y = 0$).

Panel (a) of Fig. 3 exhibits the LDOS at the center of vortex ($x = y = 0$) vs the quasiparticle energy ε , and at differing values of the exchange field: $h_0 = 0, 2\Delta, 4\Delta$,

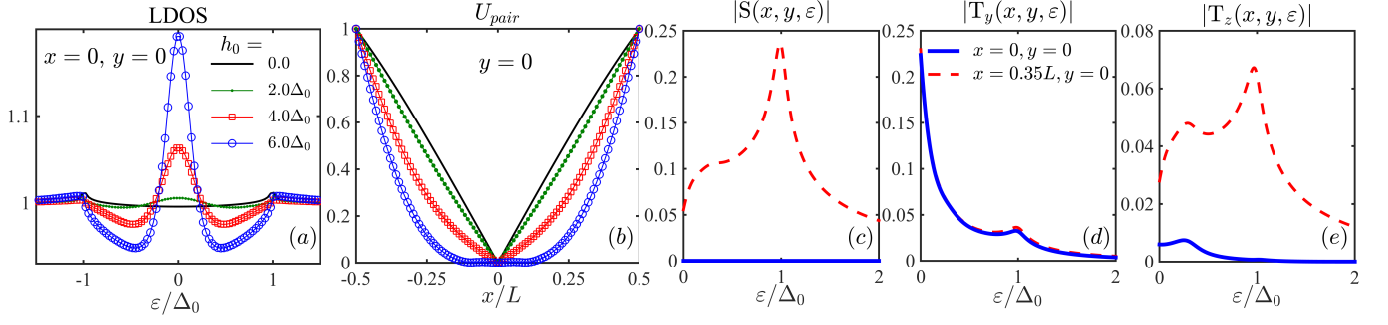


FIG. 3. (Color online) (a) Local density of states as a function of quasiparticles' energy ε at the vortex core, $x = y = 0$ (shown in Fig. 2) for four values of internal field in the Ho layers, $h_0 = 0.0, 2.0\Delta_0, 4.0\Delta_0$, and $6.0\Delta_0$. (b) Corresponding singlet pair potential, U_{pair} , along the junction length, x , in the same location as the vortex core i.e. $y = 0$. (a) and (b) panels are obtained within the *full* proximity limit and the other parameters are identical to those of Fig. 2. (c)-(e) show the modulus of singlet $|S(\varepsilon)|$, spin-1 $|T_y(\varepsilon)|$, and spin-0 $|T_z(\varepsilon)|$ triplets against ε within the *low* proximity limit. The solid lines show the correlations at the vortex core while the dashed lines correspond to a representative location outside of the vortex core: $x = 0.35L, y = 0$.

and 6Δ . Panel (b) illustrates the corresponding singlet pair potential along the junction length in the x direction (at $y = 0$). To have absolute comparisons, the parameters are kept the same as those used in Fig. 2. The normalized DOS for $h_0 = 0$ is equal to unity, corresponding to the normal phase at the vortex core as discussed in relation to Fig. 2. Switching h_0 to nonzero values immediately induces a peak at zero energy and its amplitude increases with stronger, more inhomogeneous internal fields \mathbf{h} . This follows from the fact that stronger IFMs can more effectively convert singlet correlations into triplet ones. Although not shown here, our results demonstrated a disappearance of the ZEP when \mathbf{h} is uniform and collinear. To clearly determine the type of superconducting correlations responsible for the ZEPs, one can simply consider the singlet pair potential shown in panel (b). It is apparent that U_{pair} completely vanishes at $x = 0$ where the associated LDOS is calculated in panel (a). Therefore, the results clearly demonstrate that the only nonvanishing pair correlations at $x = y = 0$ are the spin-1 triplet pairs, and therefore are responsible for the induction of the ZEPs. When the opacity of the interfaces is large enough, e.g. $\zeta = 10 - 20$, the normal and anomalous Green functions can be approximated by $|G| \sim 1$ and $|F| \ll 1$ and one can expand the Green function around the bulk solution. This regime allows for the spin parameterization of the Green function via $F(\mathbf{R}, \varepsilon) = i[S(\mathbf{R}, \varepsilon) + \boldsymbol{\tau} \cdot \mathbf{T}(\mathbf{R}, \varepsilon)]\tau_y$, as exhaustively described in Ref. 11. The Green function can then be decomposed into its singlet $S(\mathbf{R}, \varepsilon)$, spin-1 $T_y(\mathbf{R}, \varepsilon)$, and spin-0 $T_z(\mathbf{R}, \varepsilon)$ triplet components. Panels (c)-(e) illustrate the behaviour of these correlations at the vortex core ($x = y = 0$) and at $x = 0.35L, y = 0$, outside of the core. It is clearly seen that the largest nonvanishing component within low energies at the center of the vortex is the odd frequency equal spin component $T_y(\mathbf{R}, \varepsilon)$. Although we have focused on precisely the vortex core in our calculations, the spin singlet component should

be practically enough suppressed (and triplets dominate) within a circle with a radius of the magnetic penetration depth around the vortex core to experimentally reveal the predicted signatures above.

It is known that vortices in clean superconductors can host bound states that are separated in energy by an amount $\sim \Delta^2/\varepsilon_F$ [33]. These bound states yield a peak in the LDOS of a vortex core at the Fermi level [33] that was first observed in Ref. 35 and then followed up by numerous theoretical and experimental works [36–44]. These low-energy states reflect relevant details of the bulk gap structure of the superconducting state [45]. It is important to emphasize that the vortices discussed here are in the diffusive limit where the quasiparticles move in random directions after each collision with the scattering sources and ξ_S is much larger than the mean free path, thus excluding the existence of Andreev bound states at the vortex cores. To achieve optimal DOS signatures, the STM tip should be placed near the vortex core, where the odd frequency triplet correlations are revealed through an enhancement of the zero energy quasiparticle states in close vicinity of the tip. Finally, it is worth mentioning that in light of the specific system parameters used for producing spin-1 triplet correlations, the thickness of the Ho layers and the actual magnetization patterns can play important roles in the singlet to triplet conversion process [11, 14, 15]. In this work, the two Ho layers are considered identical and of thickness 10nm [11, 14, 15].

Conclusions. To summarize, motivated by recent experimental progress related to the proximity induced vortices [25], we have proposed an experimentally accessible platform that utilizes the cores of proximity vortices to isolate the equal spin triplet pairings [1, 2]. We showed that a proximity-induced vortex can be generated in the normal layer of a two dimensional diffusive S-Ho/N/Ho-S junction by applying an external magnetic field to the junction plane, with the Holmium (Ho) layers serving as sources of spin-1 triplet correlations. We then demon-

strated that one can directly probe the equal spin triplet pairings via a tunneling spectroscopy experiment at the normal core of the vortex.

M.A. would like to thank G. Sewell for his valuable instructions in the numerical parts of this work. A.Z. was financially supported by the Swedish Research Council Grant No. 642-2013-7837. K.H. is supported in part by ONR and a grant of HPC resources from the DOD HPCMP.

-
- [1] A.I. Buzdin, *Proximity effects in superconductor-ferromagnet heterostructures*, *Rev. Mod. Phys.* **77**, 935-936 (2005).
 - [2] F.S. Bergeret, A.F. Volkov, and K.B. Efetov, *Odd triplet superconductivity and related phenomena in superconductor-ferromagnet structures*, *Rev. Mod. Phys.* **77**, 1321 (2005).
 - [3] R.S. Keizer, S.T.B. Goennenwein, T.M. Klapwijk, G. Miao, G. Xiao and A. Gupta, *A spin triplet supercurrent through the half-metallic ferromagnet CrO₂*, *Nature* **439**, 825 (2006).
 - [4] K. Halterman, P.H. Barsic, and O.T. Valls, *Odd Triplet Pairing in Clean Superconductor/Ferromagnet Heterostructures*, *Phys. Rev. Lett.* **99**, 127002 (2007).
 - [5] I.V. Bobkova and A.M. Bobkov, *Long-range proximity effect for opposite-spin pairs in superconductor-ferromagnet heterostructures under nonequilibrium quasiparticle distribution*, *Phys. Rev. Lett.* **108**, 197002 (2012).
 - [6] Y.N. Khaydukov, G.A. Ovsyannikov, A.E. Sheyerman, K.Y. Constantinian, L. Mustafa, T. Keller, M.A. Uribe-Laverde, Yu.V. Kislinskii, A.V. Shadrin, A. Kalabukhov, B. Keimer, D. Winkler, *Evidence for spin-triplet superconducting correlations in metal-oxide heterostructures with noncollinear magnetization*, *Phys. Rev. B* **90**, 035130 (2014).
 - [7] A. Moor, A.F. Volkov, K.B. Efetov, *Nematic versus ferromagnetic spin filtering of triplet Cooper pairs in superconducting spintronics*, *Phys. Rev. B* **92**, 180506(R) (2015).
 - [8] A. Singh, S. Voltan, K. Lahabi, and J. Aarts, *Colossal Proximity Effect in a Superconducting Triplet Spin Valve Based on the Half-Metallic Ferromagnet CrO₂*, *Phys. Rev. X* **5**, 021019 (2015).
 - [9] M. Eschrig, *Spin-polarized supercurrents for spintronics: a review of current progress*, *Reports on Progress in Physics* **78**, 104501 (2015).
 - [10] J. Linder and J.W.A. Robinson, *Superconducting Spintronics*, *Nat. Phys.* **11**, 307 (2015).
 - [11] M. Alidoust and K. Halterman, *Proximity induced vortices and long-range triplet supercurrents in ferromagnetic Josephson junctions and spin valves*, *J. Appl. Phys.* **117**, 123906 (2015).
 - [12] S.V. Bakurskiy, N.V. Klenov, I.I. Soloviev, M.Yu. Kupriyanov and A.A. Golubov, *Superconducting phase domains for memory applications*, *Appl. Phys. Lett.* **108**, 042602 (2016).
 - [13] A.A. Golubov, M.Y. Kupriyanov, E. Il'Ichev, *The current-phase relation in Josephson junctions*, *Rev. Mod. Phys.* **76**, 411 (2004).
 - [14] J.W.A. Robinson, J.D.S. Witt and M.G. Blamire, *Controlled injection of spin-triplet supercurrents into a strong ferromagnet*, *Science*, **329**, 5987 (2010).
 - [15] M. Alidoust, J. Linder, *Spin-triplet supercurrent through inhomogeneous ferromagnetic trilayers*, *Phys. Rev. B* **82**, 224504 (2010).
 - [16] M. Houzet and A.I. Buzdin, *Long range triplet Josephson effect through a ferromagnetic trilayer*, *Phys. Rev. B* **76**, 060504(R) (2007).
 - [17] T. E. Baker, A. Richie-Halford, A. Bill, *Long Range Triplet Josephson Current and 0π Transition in Tunable Domain Walls*, *New J. Phys.* **16**, 093048 (2014).
 - [18] I. Baladie, A.I. Buzdin, *Local quasiparticle density of states in ferromagnet/superconductor nanostructures*, *Phys. Rev. B* **64**, 224514 (2001).
 - [19] S. Kawabata, Y. Asano, Y. Tanaka, and A.A. Golubov, *Robustness of Spin-Triplet Pairing and Singlet-Triplet Pairing Crossover in Superconductor/Ferromagnet Hybrids*, *J. Phys. Soc. Jap.* **82**, 124702 (2013).
 - [20] M. Alidoust, K. Halterman, and O.T. Valls, *Zero Energy Peak and Triplet Correlations in Nanoscale SFF Spin-Valves*, *Phys. Rev. B* **92**, 014508 (2015).
 - [21] T. Yokoyama, Y. Tanaka, A. A. Golubov, *Manifestation of the odd-frequency spin-triplet pairing state in diffusive ferromagnet/superconductor junctions*, *Phys. Rev. B* **75**, 134510 (2007).
 - [22] Y. Kalcheim, O. Millo, A. Di Bernardo, A. Pal, and J.W.A. Robinson, *Inverse proximity effect at superconductor-ferromagnet interfaces: Evidence for induced triplet pairing in the superconductor*, *Phys. Rev. B* **92**, 060501(R) (2015).
 - [23] S. Mironov, A. Buzdin, *Triplet proximity effect in superconducting heterostructures with a half-metallic layer*, *Phys. Rev. B* **92**, 184506 (2015).
 - [24] K. Halterman and M. Alidoust, *Half-Metallic Superconducting Triplet Spin Valve*, *Phys. Rev. B* **94**, 064503 (2016).
 - [25] D. Roditchev, C. Brun, L. Serrier-Garcia, J.C. Cuevas, V. H.L. Bessa, M.V. Milosevic, F. Debontridder, V. Stolyarov and T. Cren, *Direct observation of Josephson vortex cores*, *Nat. Phys. Lett.* **11**, 332 (2015).
 - [26] J.C. Cuevas and F.S. Bergeret, *Magnetic Interference Patterns and Vortices in Diffusive SNS Junctions*, *Phys. Rev. Lett.* **99**, 217002 (2007).
 - [27] M. Alidoust and J. Linder *φ -State and Inverted Fraunhofer Pattern in Nonaligned Josephson Junctions*, *Phys. Rev. B* **87**, 060503(R) (2013).
 - [28] A.A. Zyuzin, M. Alidoust, and D. Loss, *Josephson Junction through a Disordered Topological Insulator with Helical Magnetization*, *Phys. Rev. B* **93**, 214502 (2016).
 - [29] K.D. Usadel, *Generalized Diffusion Equation for Superconducting Alloys*, *Phys. Rev. Lett.* **25**, 507 (1977).
 - [30] N. Schopol *Transformation of the Eilenberger Equations of Superconductivity to a Scalar Riccati Equation*, [cond-mat/9804064](#); *Impurity States in D-Wave Superconductors, in Quasiclassical Methods in the Theory of Superconductivity and Superfluidity* (D. Rainer and J.A. Sauls, eds.), pp. 354, Bayreuth, Bayreuth, Germany, (1998), D.-C. Chen, D. Rainer, and J.A. Sauls.
 - [31] A.V. Zaitsev, *Zh. Eksp. Teor. Fiz.* **86**, 1742 (1984) [*Sov. Phys. JETP* **59**, 1015 (1984)]; M.Y. Kupriyanov et al., *Sov. Phys. JETP* **67**, 1163 (1988).
 - [32] I. Sosnin, H. Cho, V.T. Petrashov, and A.F. Volkov, *Su-*

- perconducting phase coherent electron transport in proximity conical ferromagnets, *Phys. Rev. Lett.* **96**, 157002 (2006).
- [33] C. Caroli, P.G. De Gennes and J. Matricon, *Bound fermion states on a vortex line in a type II superconductor*, *Phys. Lett.* **9**, 307 (1964).
- [34] M. Amundsen, J. Linder, *General solution of 2D and 3D superconducting quasiclassical systems*, *Sci. Rep.* **6**, 22765 (2016).
- [35] H.F. Hess, R.B. Robinson, R.C. Dynes, J.M. Valles, Jr., and J.V. Waszczak, *Scanning-tunneling-microscope observation of the Abrikosov flux lattice and the density of states near and inside a fluxoid*, *Phys. Rev. Lett.* **62**, 214 (1989).
- [36] J.D. Shore, M. Huang, A.T. Dorsey, and J.P. Sethna, *Density of states in a vortex core and the zero-bias tunneling peak*, *Phys. Rev. Lett.* **62**, 3089 (1989).
- [37] F. Gygi and M. Schluter, *Self-consistent electronic structure of a vortex line in a type-II superconductor*, *Phys. Rev. B* **43**, 7609 (1991).
- [38] C.-L. Song, Y.-L. Wang, P. Cheng, Y.-P. Jiang, W. Li, T. Zhang, Z. Li, K. He, L. Wang, J.-F. Jia, H. -H. Hung, C. Wu, X. Ma, X. Chen, and Q. -K. Xue, *Direct observation of nodes and twofold symmetry in FeSe superconductor*, *Science* **332**, 1410 (2011).
- [39] L. Shan, Y.-L. Wang, B. Shen, B. Zeng, Y. Huang, A. Li, D. Wang, H. Yang, C. Ren, Q.-H. Wang, S. Pan and H.-H. Wen, *Observation of Lattice and Andreev Bound States of Vortices in $\text{Ba}_{0.6}\text{K}_{0.4}\text{Fe}_2\text{As}_2$ Single Crystals with Scanning Tunneling Microscopy/Spectroscopy*, *Science* **332**, 1410 (2011).
- [40] T. Hanaguri, K. Kitagawa, K. Matsubayashi, Y. Mazaki, Y. Uwatoko, and H. Takagi, *Scanning tunneling microscopy/spectroscopy of vortices in LiFeAs*, *Phys. Rev. B* **85**, 214505 (2012).
- [41] B. Mencia Uranga, M.N. Gastiasoro1, and B.M. Andersen, *Electronic vortex structure of Fe-based superconductors: Application to LiFeAs*, *Phys. Rev. B* **93**, 224503 (2016).
- [42] D. Wulferding, I. Yang, J. Yang, M. Lee, H.C. Choi, S. L. Bud'ko, P.C. Canfield, H.W. Yeom, and J. Kim, *Spatially resolved penetration depth measurements and vortex manipulation in the ferromagnetic superconductor $\text{ErNi}_2\text{B}_2\text{C}$* , *Phys. Rev. B* **92**, 014517 (2015).
- [43] K.K. Tanaka, M. Ichioka, S. Onari, *Site-selective NMR for odd-frequency Cooper pairs around vortex in chiral p-wave superconductors*, *Phys. Rev. B* **93**, 094507 (2016).
- [44] M. Timmermans, L. Serrier-Garcia, M. Perini, J. Van de Vondel, and V.V. Moshchalkov, *Direct observation of condensate and vortex confinement in nanostructured superconductors*, *Phys. Rev. B* **93**, 054514 (2016).
- [45] A. V. Balatsky, I. Vekhter, and Jian-Xin Zhu, *Impurity-induced states in conventional and unconventional superconductors*, *Rev. Mod. Phys.* **78**, 373 (2006).